Physics Letters B 772 (2017) 854–864

Contents lists available at ScienceDirect

Physics Letters B

www.elsevier.com/locate/physletb

First measurement of the Sivers asymmetry for gluons using SIDIS data

The COMPASS Collaboration

C. Adolph [h], M. Aghasyan [y], R. Akhunzyanov [g], M.G. Alexeev [aa], G.D. Alexeev [g], A. Amoroso [aa,ab], V. Andrieux [ac,u], N.V. Anfimov [g], V. Anosov [g], A. Antoshkin [g], K. Augsten [g,s], W. Augustyniak [ad], A. Austregesilo [p], C.D.R. Azevedo [a], B. Badełek [ae], F. Balestra [aa,ab], M. Ball [c], J. Barth [d], R. Beck [c], Y. Bedfer [u], J. Bernhard [m,j], K. Bicker [p,j], E.R. Bielert [j], R. Birsa [y], M. Bodlak [r], P. Bordalo [l,1], F. Bradamante [x,y], C. Braun [h], A. Bressan [x,y], M. Büchele [i], W.-C. Chang [v], C. Chatterjee [f], M. Chiosso [aa,ab], I. Choi [ac], S.-U. Chung [p,2], A. Cicuttin [z,y], M.L. Crespo [z,y], Q. Curiel [u], S. Dalla Torre [y], S.S. Dasgupta [f], S. Dasgupta [x,y], O.Yu. Denisov [ab,*], L. Dhara [f], S.V. Donskov [t], N. Doshita [ag], Ch. Dreisbach [p], V. Duic [x], W. Dünnweber [3], M. Dziewiecki [af], A. Efremov [g], P.D. Eversheim [c], W. Eyrich [h], M. Faessler [3], A. Ferrero [u], M. Finger [r], M. Finger jr. [r], H. Fischer [i], C. Franco [l], N. du Fresne von Hohenesche [m,j], J.M. Friedrich [p], V. Frolov [g,j], E. Fuchey [u,4], F. Gautheron [b], O.P. Gavrichtchouk [g], S. Gerassimov [o,p], J. Giarra [m], F. Giordano [ac], I. Gnesi [aa,ab], M. Gorzellik [i,5], S. Grabmüller [p], A. Grasso [aa,ab], M. Grosse Perdekamp [ac], B. Grube [p], T. Grussenmeyer [i], A. Guskov [g], F. Haas [p], D. Hahne [d], G. Hamar [x,y], D. von Harrach [m], F.H. Heinsius [i], R. Heitz [ac], F. Herrmann [i], N. Horikawa [q,6], N. d'Hose [u], C.-Y. Hsieh [v,7], S. Huber [p], S. Ishimoto [ag,8], A. Ivanov [aa,ab], Yu. Ivanshin [g], T. Iwata [ag], V. Jary [s], R. Joosten [c], P. Jörg [i], E. Kabuß [m], A. Kerbizi [x,y], B. Ketzer [c], G.V. Khaustov [t], Yu.A. Khokhlov [t,9,10], Yu. Kisselev [g], F. Klein [d], K. Klimaszewski [ad], J.H. Koivuniemi [b,ac], V.N. Kolosov [t], K. Kondo [ag], K. Königsmann [i], I. Konorov [o,p], V.F. Konstantinov [t], A.M. Kotzinian [ab,11], O.M. Kouznetsov [g], M. Krämer [p], P. Kremser [i], F. Krinner [p], Z.V. Kroumchtein [g], Y. Kulinich [ac], F. Kunne [u], K. Kurek [ad], R.P. Kurjata [af], A.A. Lednev [t,27], A. Lehmann [h], M. Levillain [u], S. Levorato [y], Y.-S. Lian [v,12], J. Lichtenstadt [w], R. Longo [aa,ab], A. Maggiora [ab], A. Magnon [ac], N. Makins [ac], N. Makke [x,y], G.K. Mallot [j,*], B. Marianski [ad], A. Martin [x,y], J. Marzec [af], J. Matoušek [x,y,r], H. Matsuda [ag], T. Matsuda [n], G.V. Meshcheryakov [g], M. Meyer [ac,u], W. Meyer [b], Yu.V. Mikhailov [t], M. Mikhasenko [c], E. Mitrofanov [g], N. Mitrofanov [g], Y. Miyachi [ag], A. Nagaytsev [g], F. Nerling [m], D. Neyret [u], J. Nový [s,j], W.-D. Nowak [m], G. Nukazuka [ag], A.S. Nunes [l], A.G. Olshevsky [g], I. Orlov [g], M. Ostrick [m], D. Panzieri [ab,13], B. Parsamyan [aa,ab], S. Paul [p], J.-C. Peng [ac], F. Pereira [a], M. Pešek [r], D.V. Peshekhonov [g], N. Pierre [m,u], S. Platchkov [u], J. Pochodzalla [m], V.A. Polyakov [t], J. Pretz [d,14], M. Quaresma [l], C. Quintans [l], S. Ramos [l,1], C. Regali [i], G. Reicherz [b], C. Riedl [ac], M. Roskot [r], N.S. Rogacheva [g], D.I. Ryabchikov [t,10], A. Rybnikov [g], A. Rychter [af], R. Salac [s], V.D. Samoylenko [t], A. Sandacz [ad], C. Santos [y], S. Sarkar [f], I.A. Savin [g], T. Sawada [v], G. Sbrizzai [x,y], P. Schiavon [x,y], K. Schmidt [i,5], H. Schmieden [d], K. Schönning [j,15], E. Seder [u], A. Selyunin [g], L. Silva [l], L. Sinha [f], S. Sirtl [i], M. Slunecka [g], J. Smolik [g], A. Srnka [e], D. Steffen [j,p], M. Stolarski [l], O. Subrt [j,s], M. Sulc [k], H. Suzuki [ag,6], A. Szabelski [x,y,ad,*], T. Szameitat [i,5], P. Sznajder [ad], S. Takekawa [aa,ab], M. Tasevsky [g], S. Tessaro [y], F. Tessarotto [y], F. Thibaud [u], A. Thiel [c], F. Tosello [ab], V. Tskhay [o], S. Uhl [p], A. Vauth [j], J. Veloso [a], M. Virius [s], J. Vondra [s], S. Wallner [p], T. Weisrock [m],

http://dx.doi.org/10.1016/j.physletb.2017.07.018

M. Wilfert [m], J. ter Wolbeek [i,5], K. Zaremba [af], P. Zavada [g], M. Zavertyaev [o], E. Zemlyanichkina [g], N. Zhuravlev [g], M. Ziembicki [af], A. Zink [h]

[a] University of Aveiro, Dept. of Physics, 3810-193 Aveiro, Portugal
[b] Universität Bochum, Institut für Experimentalphysik, 44780 Bochum, Germany [16,17]
[c] Universität Bonn, Helmholtz-Institut für Strahlen- und Kernphysik, 53115 Bonn, Germany
[d] Universität Bonn, Physikalisches Institut, 53115 Bonn, Germany [16]
[e] Institute of Scientific Instruments, AS CR, 61264 Brno, Czech Republic [18]
[f] Matrivani Institute of Experimental Research & Education, Calcutta-700 030, India [19]
[g] Joint Institute for Nuclear Research, 141980 Dubna, Moscow region, Russia [20]
[h] Universität Erlangen-Nürnberg, Physikalisches Institut, 91054 Erlangen, Germany [16]
[i] Universität Freiburg, Physikalisches Institut, 79104 Freiburg, Germany [16,17]
[j] CERN, 1211 Geneva 23, Switzerland
[k] Technical University in Liberec, 46117 Liberec, Czech Republic [18]
[l] LIP, 1000-149 Lisbon, Portugal [21]
[m] Universität Mainz, Institut für Kernphysik, 55099 Mainz, Germany [16]
[n] University of Miyazaki, Miyazaki 889-2192, Japan [22]
[o] Lebedev Physical Institute, 119991 Moscow, Russia
[p] Technische Universität München, Physik Dept., 85748 Garching, Germany [16,3]
[q] Nagoya University, 464 Nagoya, Japan [22]
[r] Charles University in Prague, Faculty of Mathematics and Physics, 18000 Prague, Czech Republic [18]
[s] Czech Technical University in Prague, 16636 Prague, Czech Republic [18]
[t] State Scientific Center Institute for High Energy Physics of National Research Center 'Kurchatov Institute', 142281 Protvino, Russia
[u] IRFU, CEA, Université Paris-Saclay, 91191 Gif-sur-Yvette, France [17]
[v] Academia Sinica, Institute of Physics, Taipei 11529, Taiwan [23]
[w] Tel Aviv University, School of Physics and Astronomy, 69978 Tel Aviv, Israel [24]
[x] University of Trieste, Dept. of Physics, 34127 Trieste, Italy
[y] Trieste Section of INFN, 34127 Trieste, Italy
[z] Abdus Salam ICTP, 34151 Trieste, Italy
[aa] University of Turin, Dept. of Physics, 10125 Turin, Italy
[ab] Torino Section of INFN, 10125 Turin, Italy
[ac] University of Illinois at Urbana-Champaign, Dept. of Physics, Urbana, IL 61801-3080, USA [25]
[ad] National Centre for Nuclear Research, 00-681 Warsaw, Poland [26]
[ae] University of Warsaw, Faculty of Physics, 02-093 Warsaw, Poland [26]
[af] Warsaw University of Technology, Institute of Radioelectronics, 00-665 Warsaw, Poland [26]
[ag] Yamagata University, Yamagata 992-8510, Japan [22]

ARTICLE INFO

Article history:
Received 10 January 2017
Received in revised form 26 May 2017
Accepted 10 July 2017
Available online 19 July 2017
Editor: M. Doser

Keywords:
Deep inelastic scattering
Gluon
Sivers
TMD
PDF

ABSTRACT

The Sivers function describes the correlation between the transverse spin of a nucleon and the transverse motion of its partons. For quarks, it was studied in previous measurements of the azimuthal asymmetry of hadrons produced in semi-inclusive deep inelastic scattering of leptons off transversely polarised nucleon targets, and it was found to be non-zero. In this letter the evaluation of the Sivers asymmetry for gluons is presented. The contribution of the photon–gluon fusion subprocess is enhanced by requiring two high transverse-momentum hadrons. The analysis method is based on a Monte Carlo simulation that includes three hard processes: photon–gluon fusion, QCD Compton scattering and the leading-order virtual-photon absorption process. The Sivers asymmetries of the three processes are simultaneously extracted using the LEPTO event generator and a neural network approach. The method is applied to samples of events containing at least two hadrons with large transverse momentum from the COMPASS data taken with a 160 GeV/c muon beam scattered off transversely polarised deuterons and protons. With a significance of about two standard deviations, a negative value is obtained for the gluon Sivers asymmetry. The result of a similar analysis for a Collins-like asymmetry for gluons is consistent with zero.

* Corresponding authors.
E-mail addresses: oleg.denisov@cern.ch (O.Yu. Denisov), gerhard.mallot@cern.ch (G.K. Mallot), adam.szabelski@cern.ch (A. Szabelski).

[1] Also at Instituto Superior Técnico, Universidade de Lisboa, Lisbon, Portugal.
[2] Also at Dept. of Physics, Pusan National University, Busan 609-735, Republic of Korea and at Physics Dept., Brookhaven National Laboratory, Upton, NY 11973, USA.
[3] Supported by the DFG cluster of excellence 'Origin and Structure of the Universe' (http://www.universe-cluster.de) (Germany).
[4] Supported by the Laboratoire d'excellence P2IO (France).
[5] Supported by the DFG Research Training Group Programmes 1102 and 2044 (Germany).
[6] Also at Chubu University, Kasugai, Aichi 487-8501, Japan.
[7] Also at Dept. of Physics, National Central University, 300 Jhongda Road, Jhongli 32001, Taiwan.
[8] Also at KEK, 1-1 Oho, Tsukuba, Ibaraki 305-0801, Japan.
[9] Also at Moscow Institute of Physics and Technology, Moscow Region, 141700, Russia.
[10] Supported by Presidential Grant NSh-999.2014.2 (Russia).
[11] Also at Yerevan Physics Institute, Alikhanian Br. Street, Yerevan, Armenia, 0036.
[12] Also at Dept. of Physics, National Kaohsiung Normal University, Kaohsiung County 824, Taiwan.
[13] Also at University of Eastern Piedmont, 15100 Alessandria, Italy.

1. Introduction

An interesting and recently examined property of the quark distribution in a nucleon that is polarised transversely to its momentum is not left-right symmetric with respect to the plane defined by the directions of nucleon spin and momentum. This asymmetry of the distribution function is called the Sivers effect. It was first suggested [1] as an explanation of the large left-right single transverse spin asymmetries observed for pions produced in the reaction $p^{\uparrow}p \to \pi X$ [2–4]. Soon after, the existence of such an asymmetric distribution, known as Sivers distribution function, was excluded on the basis of T-invariance arguments [5]. Only ten years later it was recognised that such a function may indeed exist [6]. At that time it was also predicted that the Sivers function in semi-inclusive measurements of hadron production in DIS (SIDIS) and in the Drell–Yan process should have opposite sign [7], a property referred to as "restricted universality". A few years later, the Sivers effect for quarks was observed in SIDIS experiments using transversely polarised proton targets, first by the HERMES Collaboration [8] and then by the COMPASS Collaboration [9]. From combined analyses of the first HERMES data and the early COMPASS data taken with a transversely polarised deuteron target [10], first extractions of the Sivers functions for u and d-quarks emerged [11–13]. Since then, more precise measurements of the Sivers effect were performed by the HERMES [14] and COMPASS [15–17] Collaborations, and new measurements with a transversely polarised ^{3}He target were also carried out at JLab [18,19]. More information can be found in recent reviews [20–22].

At this point, the question arises whether or not the gluon distribution in a transversely polarised nucleon is also left-right asymmetric, i.e. exhibits a Sivers effect similar to that found for the quark distributions. Recently, the issue has been discussed repeatedly in the literature and the properties of the gluon Sivers distributions have been studied in great detail [23,24]. While it was found that a non-zero Sivers function implies transverse motion of partons in the nucleon, presently the connection between the Sivers function and the parton orbital angular momentum in the nucleon can only be described in a model-dependent way [25]. Originally, the correspondence between the left-right asymmetry now known as Sivers effect and parton orbital angular momentum was proposed by Sivers himself [1,26], and then it was further elaborated by several authors [27–29].

Presently, the information on the gluon Sivers function is scarce. An important theoretical constraint comes from the so-called Burkardt sum rule [30]. It states, based on the presence of QCD colour-gauge links, that the total transverse momentum of all partons in a transversely polarised proton should vanish. Fits to the Sivers asymmetry using SIDIS data [31] almost fulfil, within uncertainties, the Burkardt sum rule and hence leave little space for a gluon contribution. From the null result of the COMPASS experiment for the Sivers asymmetry of positive and negative hadrons produced on a transversely polarised deuteron target [10], together with additional theoretical considerations, it was stated [32] that the gluon contribution to parton orbital angular momentum should be negligible, and consequently that the gluon Sivers effect should be small. Also, using the so-called transverse momentum dependent (TMD) generalised parton model and the most recent phenomenological information on the quark Sivers distributions coming from SIDIS data, constraints on the gluon Sivers function were derived [33] from the recent precise data on the transverse single spin asymmetry $A_N(p^{\uparrow}p \to \pi^0 X)$ that was measured at central rapidity by the PHENIX Collaboration at RHIC [34]. Altogether, it is of great interest to know whether there exists a Sivers effect for gluons or not.

In DIS, the leading-order virtual-photon absorption subprocess (LP) does not provide direct access to the gluon distribution since the virtual photon does not couple to the gluon. Hence higher-order subprocesses have to be studied, *i.e.* QCD Compton scattering (QCDC) and Photon–Gluon Fusion (PGF). It is well known that in lepton–proton scattering one of the most promising processes to directly probe the gluon is open charm production, $\ell p^{\uparrow} \to \ell' c\bar{c}X$. This channel was studied in detail by the COMPASS Collaboration in order to measure $\Delta g/g$, *i.e.* the gluon polarisation in a longitudinally polarised nucleon [35]. Tagging the charm quark by identifying D-mesons in the final state has the advantage that in lowest order of the strong coupling constant there are no other contributions to the cross section, so that one becomes essentially sensitive to the gluon distribution function. An alternative method to tag the gluon in DIS, which was also developed and used by COMPASS is the production of high-p_T hadrons [36,37] that has the advantage of higher statistics. In the leading process, the hadron transverse momentum p_T with respect to the virtual photon direction (in the frame where the nucleon momentum is parallel to this direction) originates from the intrinsic transverse momentum k_T of the struck quark in the nucleon and its fragmentation, which both lead to a small transverse component. On the contrary, both the QCDC and PGF hard subprocesses can provide hadrons with high transverse momentum. Therefore, tagging events with hadrons of high transverse momentum p_T enhances the contribution of higher-order subprocesses. Nevertheless, although in such a high-p_T sample the PGF fraction is enriched, the contributions from LP and QCDC have to be subtracted in order to single out the contribution of the PGF subprocess to the measured asymmetry [38].

In this letter, the gluon Sivers effect is investigated using COMPASS data collected by scattering a 160 GeV/c muon beam off transversely polarised deuterons and protons. The experimental set-up and the data selection are described in Section 2. In Section 3 the measurement is described. The details of the analysis are given in Section 4. The procedure of neural network (NN) training with a Monte Carlo data sample is shown in Section 5. Section 6 contains the overview of the systematic studies. In Section 7 the results are presented. Summary and conclusions are given in Section 8.

2. Experimental set-up and data selection

The COMPASS experiment uses a fixed target set-up and the naturally polarised muon beam delivered by the M2 beam line of the CERN SPS. The transversely polarised deuteron target used in the years 2003 and 2004 was consisting of two oppositely polarised cylindrical cells situated along the beam, each 60 cm long

[14] Present address: RWTH Aachen University, III. Physikalisches Institut, 52056 Aachen, Germany.
[15] Present address: Uppsala University, Box 516, 75120 Uppsala, Sweden.
[16] Supported by BMBF – Bundesministerium für Bildung und Forschung (Germany).
[17] Supported by FP7, HadronPhysics3, Grant 283286 (European Union).
[18] Supported by MEYS, Grant LG13031 (Czech Republic).
[19] Supported by SAIL (CSR) and B. Sen fund (India).
[20] Supported by CERN–RFBR Grant 12-02-91500.
[21] Supported by FCT – Fundo Regional para a Ciência e Tecnologia, COMPETE and QREN, Grants CERN/FP 116376/2010, 123600/2011 and CERN/FIS-NUC/0017/2015 (Portugal).
[22] Supported by MEXT and JSPS, Grants 18002006, 20540299 and 18540281, the Daiko and Yamada Foundations (Japan).
[23] Supported by the Ministry of Science and Technology, Taiwan (Taiwan).
[24] Supported by the Israel Academy of Sciences and Humanities (Israel).
[25] Supported by NSF – National Science Foundation (USA).
[26] Supported by NCN, Grant 2015/18/M/ST2/00550 (Poland).
[27] Deceased.

with a 10 cm gap in between. In 2010, the transversely polarised proton target consisted of three cells, 30 cm, 60 cm and 30 cm long with 5 cm gaps between them. The polarisation direction in the central cell was opposite to that in the downstream and upstream cells. During all data taking periods, the polarisation direction was reversed once per week in order to minimise systematic effects due to acceptance. For the measurements using a deuteron target the cells were filled with ^{6}LiD. The ^{6}Li nucleus can be regarded to be composed of a quasi-free deuteron and a ^{4}He core. The average dilution factor f_d, which is defined as ratio of the DIS cross section for only the polarisable nucleons in the target over the DIS cross section for all target nucleons, amounts to 0.36 including also electromagnetic radiative corrections. The average deuteron polarisation was 0.50. For the measurements using a proton target, the cells were filled with NH_3. The average dilution factor f_p amounts to 0.15 and the average proton polarisation was 0.80. A muon beam energy of 160 GeV/c was chosen for all measurements. The basic features of the COMPASS spectrometer, as described in Ref. [40], are the same for 2003–2004 and 2010 data taking. Several upgrades were performed in 2005, where the main one was the installation of a new target magnet that allowed us to increase the polar angle acceptance from 70 mrad to 180 mrad.

A crucial point of this analysis is the search for an observable that is strongly correlated with the azimuthal angle ϕ_g of the gluon. In the MC simulations using the LEPTO generator [41], gluons are probed through the PGF subprocess that has a quark–antiquark pair in the final state, and the fragmentation process is described by the Lund model [42]. As a result of MC studies, the best correlation is found between ϕ_g and ϕ_P, where the latter denotes the azimuthal angle of the vector sum $\boldsymbol{P}$ of the two hadron momenta. For the present analysis, two charged hadrons are selected in each event. If more than two charged hadrons are reconstructed in an event, only the hadron with the largest transverse momentum, p_{T1}, and the one with the second-largest transverse momentum, p_{T2}, are taken into account. In order to enhance the PGF fraction in the sample and at the same time the correlation between ϕ_g and ϕ_P, further requirements are applied to the transverse momenta of the two hadrons, *i.e.* $p_{T1} > 0.7$ GeV/c and $p_{T2} > 0.4$ GeV/c. Moreover, the fractional energies of the two hadrons must fulfil the conditions $z_i > 0.1$ $(i = 1, 2)$ and $z_1 + z_2 < 0.9$, where the last requirement rejects events from diffractive vector-meson production. Hadron pairs are selected without constraining their charge. With the above choice the correlation coefficient amounts to 0.54. The Sivers asymmetry is obtained as the sine modulation in the Sivers angle, which is defined as $\phi_{Siv} = \phi_P - \phi_S$ in this analysis. Here, ϕ_S is the azimuthal angle of the nucleon spin vector.

The same kinematic data selection is used for both deuteron and proton data. The requirement on photon virtuality, $Q^2 > 1$ (GeV/c)^2, selects events in the perturbative region of QCD. The requirement on the mass of the hadronic final state, $W > 5$ GeV/c^2, removes the region of exclusive nucleon resonance production. The Bjorken-x variable covers the range $0.003 < x_{Bj} < 0.7$. The fractional energy of the virtual photon, y, is limited by $y > 0.1$ to remove a region sensitive to experimental biases and by $y < 0.9$ to events with large electromagnetic radiative corrections.

3. Sivers asymmetry in two-hadron production

In order to extract the gluon Sivers asymmetry, two-hadron events produced in muon-nucleon scattering, $\mu + N \to \mu' + 2h + X$, are selected as described in Section 2. By labelling with the symbol $d^7\sigma\uparrow$ ($d^7\sigma\downarrow$) the cross section for events that were produced using a target cell with polarisation direction upwards (downwards) in the laboratory, the Sivers asymmetry can be written as

$$A_T^{2h}(\vec{x}, \phi_{Siv}) = \frac{\Delta\sigma(\vec{x}, \phi_{Siv})}{\sigma(\vec{x})}, \tag{1}$$

where $\vec{x} = (x_{Bj}, Q^2, p_{T1}, p_{T2}, z_1, z_2)$, $\Delta\sigma \equiv d^7\sigma\uparrow - d^7\sigma\downarrow$ and $\sigma \equiv d^7\sigma\uparrow + d^7\sigma\downarrow$. All cross sections are integrated over the two azimuthal angles ϕ_S and ϕ_R, where ϕ_R is the azimuthal angle of the vector difference $\boldsymbol{R} = \boldsymbol{P}_1 - \boldsymbol{P}_2$, which describes the relative momentum of the two hadrons. The number of events in a ϕ_{Siv} bin is given by

$$N(\vec{x}, \phi_{Siv}) = \alpha(\vec{x}, \phi_{Siv})\left(1 + f(\vec{x}) P_T A^{Siv}(\vec{x}) \sin\phi_{Siv}\right). \tag{2}$$

Here $f(\vec{x})$ is the dilution factor, P_T the target polarisation and $\alpha = an\Phi\sigma_0$ an acceptance-dependent factor, where a is the total spectrometer acceptance, n the density of scattering centres, Φ the beam flux and σ_0 the spin-averaged part of the cross section. From here on, the Sivers asymmetry $A_T^{2h}(\vec{x}, \phi_{Siv})$ is factorised into the azimuth-independent amplitude $A^{Siv}(\vec{x})$ and the modulation $\sin\phi_{Siv}$.

In order to evaluate the Sivers asymmetry of the gluon, the amplitude of the $\sin\phi_{Siv}$ modulation is extracted from the data. The general expression for the cross section of SIDIS production with at least one hadron in the final state is well known [43]. It contains eight azimuthal modulations, which are functions of the single-hadron azimuthal angle and ϕ_S. In the absence of correlations possibly introduced by experimental effects, all eight are orthogonal. The Sivers asymmetry can either be extracted by fitting only the amplitude of the $\sin\phi_{Siv}$ modulation or one can perform a simultaneous fit of all eight amplitudes. In the case of heavy-quark pair and dijet production in lepton–nucleon collisions, all azimuthal asymmetries associated to the gluon distribution function have been recently worked out in Ref. [44]. There, the Sivers asymmetry is defined as the amplitude of the $\sin(\phi_T - \phi_S)$ modulation, where ϕ_T is the azimuthal angle of the transverse-momentum vector of the quark–antiquark pair, $\boldsymbol{q}_T$. In our analysis, ϕ_T is replaced by ϕ_P exploiting its correlation with the gluon azimuthal angle ϕ_g, and the Sivers asymmetry is extracted taking into account only the $\sin(\phi_P - \phi_S)$ modulation in the cross section. It was verified that including in the cross section the same eight transverse-spin modulations as in SIDIS single-hadron production [43] and fitting all eight amplitudes simultaneously leads to the same result on the gluon Sivers asymmetry.

In order to determine the gluon Sivers asymmetry from two-hadron production in SIDIS, it is necessary to assume that the main contributors to muon-nucleon DIS are the three subprocesses (Fig. 1) as presented in Ref. [41]. This model is successful in describing the unpolarised data. At COMPASS kinematics, the leading process appears at zero-order QCD in the total DIS cross section and it is the dominant subprocess, while the other two subprocesses, photon–gluon fusion and QCD Compton, are first-order QCD processes and hence suppressed. However, their contribution can be enhanced by requiring high transverse momentum of the produced hadrons, as mentioned above.

Introducing the subprocess fractions $R_j = \sigma_j/\sigma$ ($j \in$ {PGF, QCDC, LP}), the amplitude of the Sivers asymmetry can be expressed in terms of the amplitudes of the three contributing subprocesses:

$$\begin{aligned} f P_T A^{Siv} \sin\phi_{Siv} &= \frac{\Delta\sigma}{\sigma} = \frac{\sigma_{\mathrm{PGF}}}{\sigma}\frac{\Delta\sigma_{\mathrm{PGF}}}{\sigma_{\mathrm{PGF}}} + \frac{\sigma_{\mathrm{QCDC}}}{\sigma}\frac{\Delta\sigma_{\mathrm{QCDC}}}{\sigma_{\mathrm{QCDC}}} + \frac{\sigma_{\mathrm{LP}}}{\sigma}\frac{\Delta\sigma_{\mathrm{LP}}}{\sigma_{\mathrm{LP}}} \\ &= f P_T (R_{\mathrm{PGF}} A^{Siv}_{\mathrm{PGF}} + R_{\mathrm{QCDC}} A^{Siv}_{\mathrm{QCDC}} + R_{\mathrm{LP}} A^{Siv}_{\mathrm{LP}}) \sin\phi_{Siv}, \end{aligned} \tag{3}$$

with $\sigma = \sum_j \sigma_j$, $\Delta\sigma = \sum_j \Delta\sigma_j$ and $f P_T A_j^{Siv} \sin\phi_{Siv} = \Delta\sigma_j/\sigma_j$. The subprocess fractions R_j are determined on an event-by-event

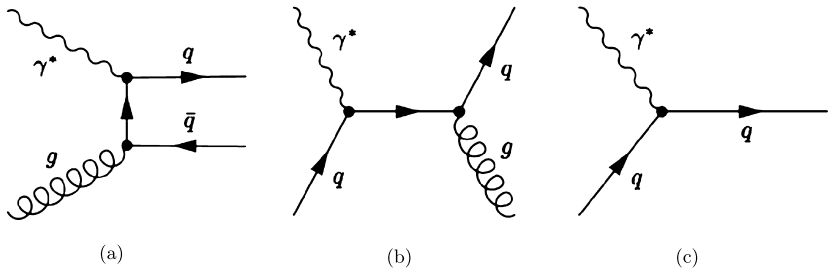

Fig. 1. Feynman diagrams considered for $\gamma^* N$ scattering: a) photon–gluon fusion (PGF), b) gluon radiation (QCD Compton scattering), c) Leading order process (LP).

basis using neural networks (NNs) trained on Monte Carlo data, as will be described in Section 5.

4. Asymmetry extraction using the methods of weights

The method adopted in the present analysis was already applied to extract the gluon polarisation from the longitudinal double-spin asymmetry in the SIDIS measurement of single-hadron production [38]. While the method may appear somewhat complex, the basic idea behind is rather simple. Equation (3) contains three unknowns, *i.e.* the asymmetries A_j^{Siv}, so that for a solution at least three equations of the type of Eq. (3) are needed. These three equations are constructed using the weighting procedure described in this section, which in addition allows us to achieve a nearly optimal statistical accuracy (in the sense of the Cramer–Rao bound [39]) in a multidimensional analysis.

Both for the deuteron data (two target cells) and the proton data (three target cells), four target configurations can be introduced. In the case of the two-cell target: 1 – upstream, 2 – downstream, 3 – upstream′, 4 – downstream′. In the case of the three-cell target: 1 – (upstream + downstream), 2 – centre, 3 – (upstream′ + downstream′), 4 – centre′. Here upstream′, centre′ and downstream′ denote the cells after the polarisation reversal and configuration 1 has the polarisation pointing upwards in the laboratory. When decomposing the Sivers asymmetry into the asymmetries of the contributing subprocesses (Eq. (3)) and introducing the Sivers modulation

$$\beta_j^t(\vec{x},\phi_{\rm Siv}) = R_j(\vec{x}) f(\vec{x}) P_T^t \sin\phi_{\rm Siv}, \tag{4}$$

which is specific for subprocess j, one can rewrite Eq. (2):

$$N^t(\vec{x},\phi_{\rm Siv}) = \alpha^t(\vec{x},\phi_{\rm Siv})\Big(1 + \beta^t_{\rm PGF}(\vec{x},\phi_{\rm Siv}) A^{Siv}_{\rm PGF}(\vec{x}) + \beta^t_{\rm QCDC}(\vec{x},\phi_{\rm Siv}) A^{Siv}_{\rm QCDC}(\vec{x}) + \beta^t_{\rm LP}(\vec{x},\phi_{\rm Siv}) A^{Siv}_{\rm LP}(\vec{x})\Big). \tag{5}$$

Here $t = 1, 2, 3, 4$ denotes the target configuration.

In order to minimise the statistical uncertainties for each subprocess, a weighting factor is introduced. It is known [45] that the choice $\omega_j = \beta_j$ for the weight optimises the statistical uncertainty but variations of the target polarisation P_T over time may introduce a bias to the final result. Therefore, the weighting factor

$$\omega_j(\vec{x}) = R_j(\vec{x}) f(\vec{x}) \sin\phi_{\rm Siv} \tag{6}$$

is used instead. By weighting each of the four equations (5) three times with ω_j depending on the subprocess $j \in \{\text{PGF, QCDC, LP}\}$, and by integrating over $\phi_{\rm Siv}$ and $\vec{x}$, twelve observed quantities q_j^t are obtained:

$$\begin{aligned} q_j^t &= \int d\vec{x} d\phi_{\rm Siv} \omega_j(\vec{x},\phi_{\rm Siv}) N^t(\vec{x},\phi_{\rm Siv}) \\ &= \tilde{\alpha}_j^t \Big(1 + \{\beta^t_{\rm PGF}\}_{\omega_j} \{A^{Siv}_{\rm PGF}\}_{\beta_{\rm PGF}\omega_j} + \{\beta^t_{\rm QCDC}\}_{\omega_j} \{A^{Siv}_{\rm QCDC}\}_{\beta_{\rm QCDC}\omega_j} \\ &\quad + \{\beta^t_{\rm LP}\}_{\omega_j} \{A^{Siv}_{\rm LP}\}_{\beta_{\rm LP}\omega_j}\Big), \end{aligned} \tag{7}$$

where $\tilde{\alpha}_j^t$ is the ω_j-weighted acceptance-dependent factor. The quantities $\{\beta_i^t\}_{\omega_j}$ and $\{A_i^{\rm Siv}\}_{\beta_i^t\omega_j}$ are weighted averages:

$$\{\beta\}_\omega = \frac{\int \alpha\beta\omega d\vec{x} d\phi_{\rm Siv}}{\int \alpha\omega d\vec{x} d\phi_{\rm Siv}}, \qquad \{A\}_{\beta\omega} = \frac{\int A\alpha\beta\omega d\vec{x} d\phi_{\rm Siv}}{\int \alpha\beta\omega d\vec{x} d\phi_{\rm Siv}}. \tag{8}$$

The acceptance factors $\tilde{\alpha}_j^t$ cancel if for the asymmetry extraction the double ratio

$$r_j := \frac{q_j^1 q_j^4}{q_j^2 q_j^3} \tag{9}$$

is used, as the data taking was performed in such a way that $\tilde{\alpha}_j^1\tilde{\alpha}_j^4/\tilde{\alpha}_j^2\tilde{\alpha}_j^3 = 1$. If this condition is not fulfilled, false asymmetries may occur. It is checked that this is not the case (see Section 6).

In this analysis, an unbiased estimator of q_j^t is selected:

$$q_j^t = \sum_{k=1}^{N_t} \omega_j^k, \tag{10}$$

and β_i^t is approximated by

$$\{\beta_i^t\}_{\omega_j} \approx \frac{\sum_{k=1}^{N^t} \beta_i^{t,k}\omega_j^k}{\sum_{k=1}^{N^t} \omega_j^k}. \tag{11}$$

This approximation holds for small observed raw asymmetries, *i.e.* $\beta A \ll 1$. It can lead to a bias of the order of $dA/A \approx 0.2\langle\beta^2\rangle$, $\langle\beta^2_{PGF}\rangle \approx 4\times10^{-6}$, which is negligible compared to other sources of systematic uncertainties, see Table 1. In order to avoid numerical inconsistencies in Eq. (11) due to a zero-pole when integrating over the full range of $\phi_{\rm Siv}$,[28] two bins in $\phi_{\rm Siv}$ ($[0;\pi]$, $[\pi;2\pi]$) are introduced. In the aforementioned three double ratios given in Eq. (9) only asymmetries are unknown. However, in order to solve the system of equations one needs to assume that the weighted asymmetry for a given subprocess i is the same for the three different weights $\omega_j\beta_i$, *i.e.* $\{A_i\}_{\beta_i\omega_{\rm PGF}} = \{A_i\}_{\beta_i\omega_{\rm QCDC}} = \{A_i\}_{\beta_i\omega_{\rm LP}}$. This means that the values of ω_j and A_i must be uncorrelated. For example, since ω_j is proportional to R_j, which in turn strongly depends on the hadron transverse momentum, one has to use a kinematic region where the asymmetries A_i are expected to be independent of p_T. Under these assumptions, the number of unknown weighted asymmetries is three, which exactly corresponds to the number of equations of type (9). These equations are solved by a χ^2 fit that includes simultaneously both bins in $\phi_{\rm Siv}$.

Assuming that A_i can be approximated by a linear function of x_i and that x_i is not correlated with ω_j, results in

[28] Note that ω_j^k, which contains $\sin\phi_{\rm Siv}$, is integrated over the region 0 to 2π.

Table 1
Summary on systematic uncertainties of the final values of the gluon Sivers asymmetry for deuteron and proton data.

Source	Deuteron data		Proton data	
	Uncertainty	Fraction of σ_{stat}	Uncertainty	Fraction of σ_{stat}
Monte Carlo settings	0.060	40%	0.054	64%
Radiative corrections	0.018	12%	0.018	21%
One or two x_{Bj} bins	0.07	47%	0.011	13%
Include 7 other asymmetries	0.003	2%	0.005	6%
Target polarisation	0.0075	5%	0.0043	5%
Dilution factor	0.003	2%	0.0018	2%
Total $\sqrt{\sum \sigma_i^2}$	0.10	63%	0.06	69%

$$\{A_i\}_{\beta_i\omega_i} = A_i(\{x_i\}_{\beta_i\omega_i}). \tag{12}$$

This approximation allows to interpret the obtained results as an asymmetry value measured at the weighted value of x_i. For each subprocess, the weighted value of x_i is obtained from MC using the relation

$$\{x_i\}_{\beta_i\omega_i} = \frac{\sum_{k=1}^{N_i} x_i^k \beta_i^k \omega_i^k}{\sum_{k=1}^{N_i} \beta_i^k \omega_i^k}. \tag{13}$$

Here, N_i is the number of events of type i in the MC data. The assumption that the values of x_i are not correlated with ω_j, which allows us to consider only $\{x_i\}_{\omega_i\beta_i}$, was verified using MC data. The details of the analysis are given in [46].

5. Monte Carlo optimisation and neural network training

The present analysis is very similar to the one used for the $\Delta g/g$ extraction using high-p_T hadron pairs [37] and single hadrons [38]. The package NetMaker [47] is used for the NN training with input, output and target vector. The NN is trained using a Monte Carlo sample with subprocess identification. The subprocess type defines the target vector. The following six kinematic variables are chosen as input vector: x_{Bj}, Q^2, p_{T1}, p_{T2}, p_{L1}, p_{L2}. The latter two are the longitudinal components of the hadron momenta. The trained neural network is applied to the data by taking as input vector of the aforementioned six variables, and its output vector is interpreted as probabilities that the given event is a result of one of the three contributing subprocesses. Hence the simulated distributions of these variables need to be in agreement with the corresponding distributions in the data.

Using the LEPTO generator (version 6.5) [41], two separate MC data samples were produced to simulate the deuteron and proton data. The generator is tuned to the COMPASS data sample obtained with the high-p_T hadron-pair selection as described in Ref. [37]. The MSTW08 parametrisation of input PDFs [48] was chosen as it gives a good description of the structure function F_2 in the COMPASS kinematic range, and it is valid down to $Q^2 = 1$ (GeV/c)^2. Electromagnetic radiative corrections [49] were applied as a weighting factor to the MC distributions shown in Figs. 2 and 3 but not in the MC samples used in NN training. This difference was studied and it was estimated to be negligible. The

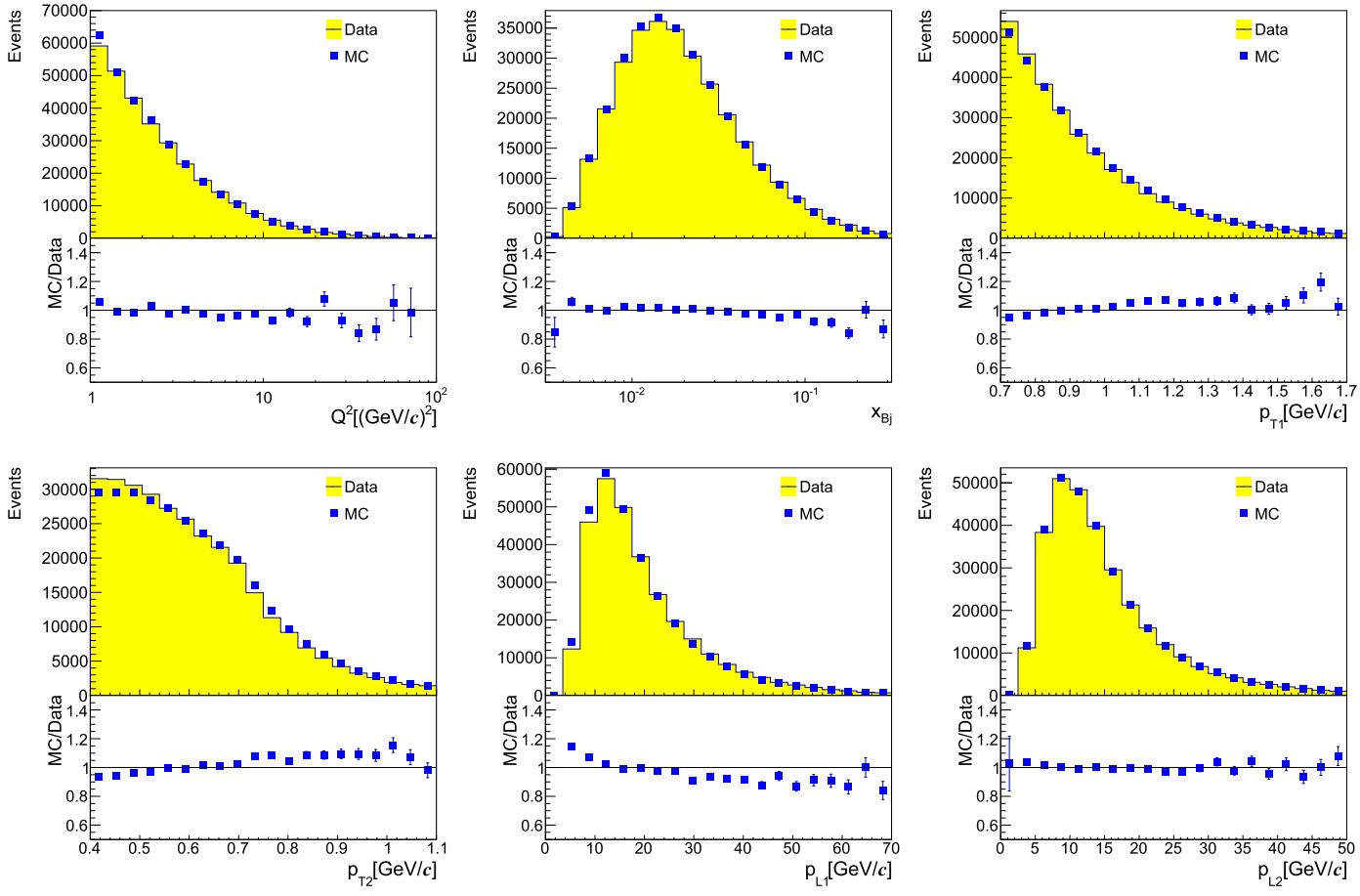

Fig. 2. Comparison of distributions of kinematic variables between experimental and MC high-p_T deuteron data.

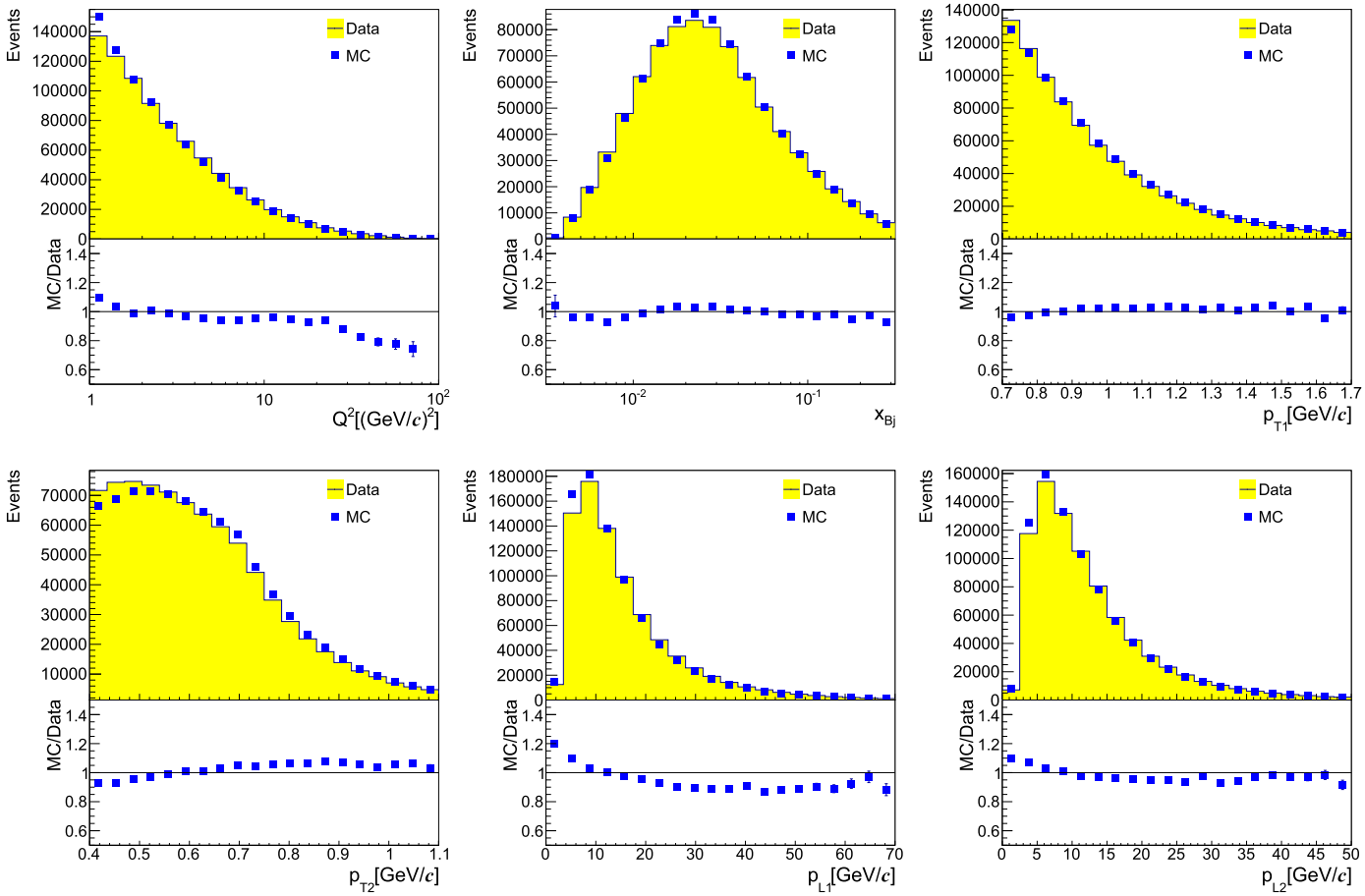

Fig. 3. Comparison of distributions of kinematic variables between experimental and MC high-p_T proton data.

generated events were processed by COMGEANT, the COMPASS detector simulation program based on GEANT3. The MC samples for the proton and deuteron data differ in the target material and in the spectrometer set-up. The FLUKA package [50] is used in order to simulate secondary interactions. As the next step, the COMPASS reconstruction program CORAL was applied. For MC data, the same data selection as for real events was used. The comparison between experimental and MC distributions of the variables used in the NN training, *i.e.* x_{Bj}, Q^2, p_{T1}, p_{T2}, p_{L1}, p_{L2}, is shown in Figs. 2 and 3 for deuteron and proton data, respectively. Discrepancies between the MC and experimental data kinematical distributions are seen at the level of 10%, mostly in the regions where statistics is small.

The main goal of the NN parametrisation is the estimation of the subprocess fractions R_j. In the typical case of signal and background separation, the expected NN output would be set to one for the signal and zero for the background. The output value returned by the NN would then correspond to the fraction of signal events in the sample at the given phase space point of the input parameter vector. In the present analysis, the subprocess fractions were estimated simultaneously. In order to have a closure relation on the subprocess probabilities, their sum must add up to one and hence only two independent output variables are needed from the NN. The estimation of the subprocess fractions R^j from the NN output is accomplished by assigning to each event the probabilities $P^{\mathrm{PGF}}_{\mathrm{NN}}$, $P^{\mathrm{QCDC}}_{\mathrm{NN}}$ and $P^{\mathrm{LP}}_{\mathrm{NN}}$. The distribution of the NN output after training is shown in Fig. 4 in the "Mandelstam representation", *i.e.* as points in an equilateral triangle with unit height. As there are three subprocesses, ideal separation would mean that a

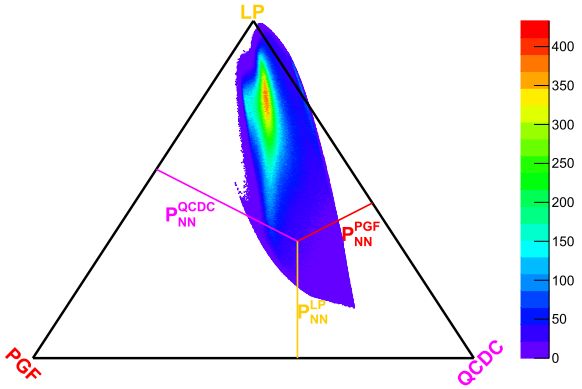

Fig. 4. Neural network output after training the MC sample for the proton analysis shown on a equilateral triangle of unit height. Vertices represent the perfect identification of the subprocesses. To each point, which represent an experimental event, three probabilities are assigned. The probability of each subprocess P^j_{NN} for a point is given by its distance to the side opposite to the vertex j of the triangle as in the "Mandelstam representation". This is illustrated by the coloured lines representing probabilities assigned to an arbitrary point.

given event is located in one of the vertices, *i.e.* belongs to one of the subprocesses. This is not the case in general, instead all information obtained from the neural network for a given event consists of the three probabilities P^{PGF}_{NN}, P^{QCDC}_{NN}, P^{LP}_{NN}, which add up to unity. In the figure, the probability P^j_{NN} is the distance between the point representing the given event and the side of the triangle opposite to the vertex representing the subprocess j

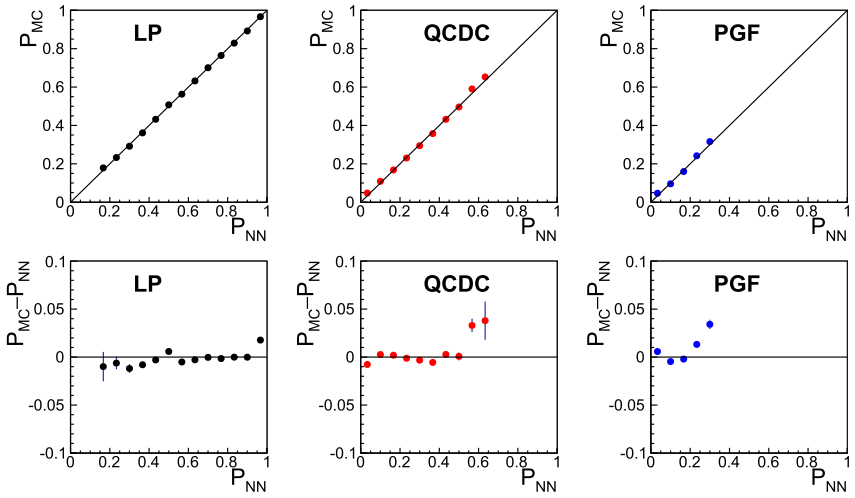

Fig. 5. Top panels: Neural network validation. Here P_{NN} is the fraction of the subprocess given by the NN and P_{MC} is the true fraction of each subprocess from MC in a given P_{NN} bin. Bottom panels: Difference $P_{MC}-P_{NN}$ per bin.

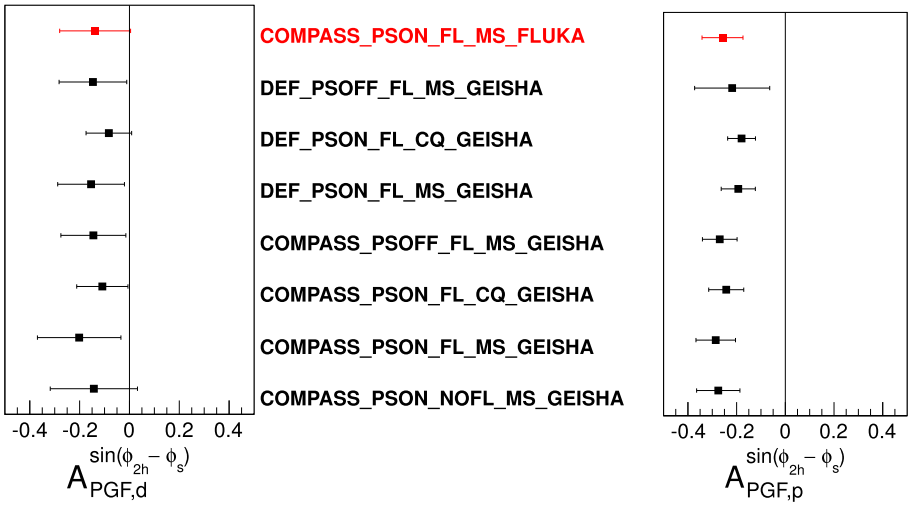

Fig. 6. Systematic changes in the final result caused by using different MC settings. Besides the final result shown on the top, seven other results are shown that are obtained with MC samples that differ by the choice of COMPASS or default LEPTO tuning, 'Parton Shower' on or off, F_L from LEPTO or from $R=\sigma_L/\sigma_T$, MSTW or CTEQ5L PDF sets, FLUKA or GHEISHA for secondary interactions. The results for deuteron(proton) data are shown in the left (right) panel.

(see coloured lines in Fig. 4). When points fall outside the triangle, one estimator was negative. This is possible because in the training the estimators are not bound to be positive. The values of the resulting three probabilities are taken as the subprocess fractions R_{PGF}, R_{QCDC} and R_{LP} in the data analysis described in Section 4.

For the validation of the NN training, a statistically independent MC sample is used to check how the NN works on a sample different from the one used for the training. In each bin of P_{NN} (the value assigned to every MC event by the trained NN), the true fraction obtained from LEPTO based on the subprocess ID, P_{MC}, is calculated. The results for the NN trained with a MC sample for the proton data are presented in Fig. 5. Altogether, the agreement between P_{NN} and P_{MC} for all three subprocesses is satisfactory. However, for the two last bins of PGF, the two last bins of QCDC and the last bin of LP the neural network output does not coincide with the true fraction of the given subprocess. As this discrepancy applies only to a small part of the event sample, it is included as a part of the MC-dependent systematic uncertainty.

6. Systematic uncertainties

The main source of systematic uncertainties is the dependence of the final results on settings and tuning of the Monte Carlo simulation. In order to estimate this uncertainty, different MC settings were used in the process of neural network training. Two different combinations of fragmentation parameters were used, *i.e.* default LEPTO tuning or COMPASS tuning for the high-p_T selected sample. The event generation was done with and without 'Parton Shower' [51]. Two PDF sets were used (MSTW08 or CTEQ5L [52]). Two different parametrisations of the longitudinal structure function F_L are used, either the one from LEPTO or the one used for the $R=\sigma_L/\sigma_T$ parametrisation of Ref. [53]. For secondary interactions, either the FLUKA or the GHEISHA [54] package were used.

Fig. 6 shows the resulting gluon Sivers asymmetries, as obtained when using eight different MC productions for deuteron and proton data. The results shown in the top row are chosen to be the final ones, as they yield the best comparison between experimental and MC data, which is shown in Figs. 2 and 3. The settings used here are FLUKA and Parton Shower, F_L from LEPTO

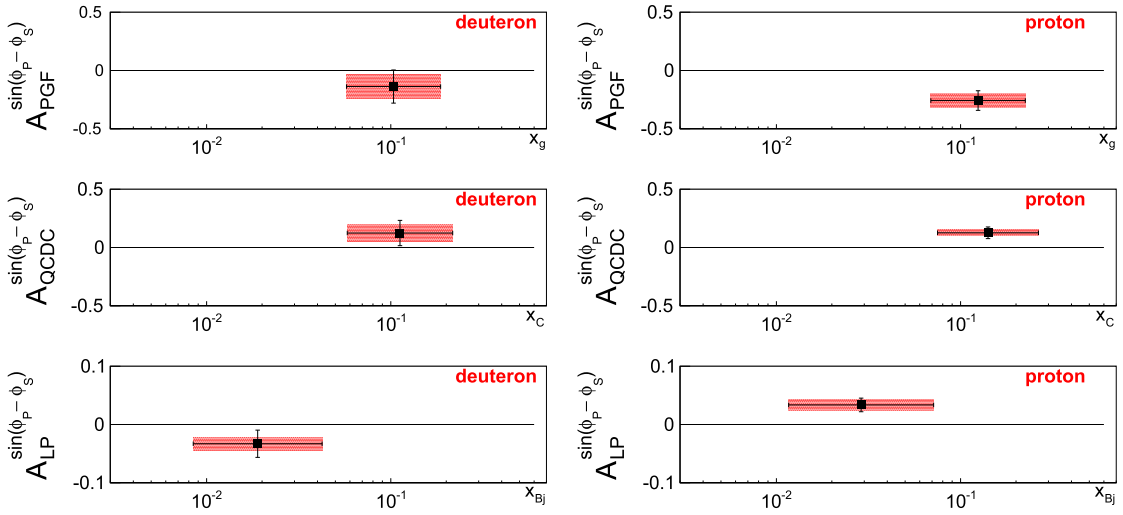

Fig. 7. Sivers two-hadron asymmetry extracted for Photon–Gluon fusion (PGF), QCD Compton (QCDC) and Leading Process (LP) from the COMPASS high-p_T deuteron (left) and proton (right) data. The x range is the RMS of the logarithmic distribution of x in the MC simulation. The red bands indicate the systematic uncertainties. Note the different ordinate scale used in the third row of panels. (For interpretation of the references to colour in this figure legend, the reader is referred to the web version of this article.)

and MSTW08 PDFs. The systematic uncertainty originating from different MC tunings is calculated as $(A^{\mathrm{PGF}}_{max} - A^{\mathrm{PGF}}_{min})/2$.

The systematic uncertainty due to false asymmetries was studied by extracting asymmetries between two parts of the same target cell. The results are found to be compatible with zero. Furthermore, it was checked how a small artificial false amplitude of the $\sin\phi_g - \phi_S$ modulation in the MC production influences the final result. When a false asymmetry of 1% is introduced, for both proton and deuteron data the final result changes by 25% of the statistical uncertainty. No systematic uncertainty is assigned to account for false asymmetries.

The final state of the photon–gluon-fusion process is a quark–antiquark pair. Thus for most hadron pairs produced from this subprocess the two hadrons should have opposite charge. Although a selection $q_1 q_2 = -1$ slightly increases the (ϕ_g, ϕ_P) correlation, it also reduces statistics. The results with and without this requirement are statistically consistent. The requirement of opposite charges of the two hadrons is hence not included in the data selection.

Radiative corrections were not included in the MC production that is used in the main analysis of this letter. In order to estimate the systematic uncertainty introduced by this omission, a separate MC sample is used that was produced for the 2006 COMPASS set-up including radiative corrections based on RADGEN [55]. The difference in the final value for the gluon Sivers asymmetry for the proton is 0.018, which corresponds to 21% of the statistical uncertainty. A corresponding systematic uncertainty is assigned to account for the fact that radiative corrections are not included in the MC simulations and hence in the NN training.

Our results are obtained in only one x_g bin for $A^{\mathrm{Siv}}_{\mathrm{PGF}}$, one x_C bin for $A^{\mathrm{Siv}}_{\mathrm{QCDC}}$ and one x_{Bj} bin for $A^{\mathrm{Siv}}_{\mathrm{LP}}$. As the asymmetries are strongly correlated, a binning in x_{Bj} affects the values of $A^{\mathrm{Siv}}_{\mathrm{PGF}}$ and $A^{\mathrm{Siv}}_{\mathrm{QCDC}}$, which are extracted in a single bin as before. The result on $A^{\mathrm{Siv}}_{\mathrm{PGF}}$ changes by 0.07 for deuteron data and 0.011 for proton data when two x_{Bj} bins are introduced, and these values are taken as an estimate of the related systematic uncertainty (see Table 1).

The asymmetries A^{Siv}_j of Eq. (5) were also extracted using the unbinned maximum likelihood method, which yields as expected, the same results for A_{PGF} as the above described analysis. Concerning the orthogonality of different modulations of the cross section, it was checked by what amount the Sivers asymmetry changes, when also the other seven asymmetries were included in the fit (see above). The change in the final value of the PGF asymmetry is negligible for both deuteron and proton data.

The systematic multiplicative uncertainties on target polarisation and dilution factor are estimated to be about 5% and 2% of the statistical uncertainty, respectively. The final systematic uncertainty is obtained by summing all components in quadrature. All above mentioned contributions and the final systematic uncertainty are listed in Table 1.

7. Results and discussion

The method of weighted asymmetries described in Section 4 was applied to the deuteron and proton data sets described in Section 2, using trained neural networks as described in Section 5. The results on the gluon Sivers asymmetry as extracted from lepton nucleon SIDIS, with at least two detected high-p_T hadrons, is shown in Fig. 7 and presented in Table 2 together with the contributions of the two other hard subprocesses, *i.e.* QCD Compton and leading process. The result of the analysis of the deuteron data is $A^{Siv,d}_{PGF} = -0.14 \pm 0.15(\mathrm{stat.}) \pm 0.10(\mathrm{syst.})$ measured at $\langle x_g \rangle = 0.13$. The proton result, $A^{Siv,p}_{PGF} = -0.26 \pm 0.09(\mathrm{stat.}) \pm 0.06(\mathrm{syst.})$ obtained at $\langle x_g \rangle = 0.15$, is consistent with the deuteron result within less than one standard deviation of the combined statistical uncertainty. The two results are expected to be consistent, as presumably the transverse motion of gluons is the same in neutron and proton. Combining the proton and deuteron results, the measured effect is negative, $A^{Siv}_{PGF} = -0.23 \pm 0.08(\mathrm{stat}) \pm 0.05(\mathrm{syst})$, which is away from zero by more than two standard deviations of the quadratically combined uncertainty. This result appears particularly interesting in view of the gluon contribution to the proton spin, as a non-zero gluon Sivers effect is a signature of gluon orbital angular momentum in the proton [25]. While the recent analysis of the PHENIX data [33] yields a gluon Sivers effect for the proton that is compatible with zero, the COMPASS result for the proton is negative and more than two standard deviations below zero. The two results may not be directly comparable, as they are obtained at different values of centre of mass energy and x_g. It may also be important to recall that the existence of colour gauge links complicates the picture, as they lead to two different universal gluon Sivers functions, which combine with process-dependent calculable factors in the two processes [56]. As a result, the gluon Sivers

Table 2
Summary of Sivers asymmetries, A^{Siv}_{PGF}, A^{Siv}_{QCDC}, A^{Siv}_{LP}, obtained for deuteron and proton data.

Subprocess	Deuteron data			Proton data		
	Asymmetry	Statistical error	Systematic uncertainty	Asymmetry	Statistical error	Systematic uncertainty
PGF	−0.14	0.15	0.10	−0.26	0.09	0.06
QCDC	0.12	0.11	0.08	0.13	0.05	0.03
LP	−0.03	0.02	0.01	0.03	0.01	0.01

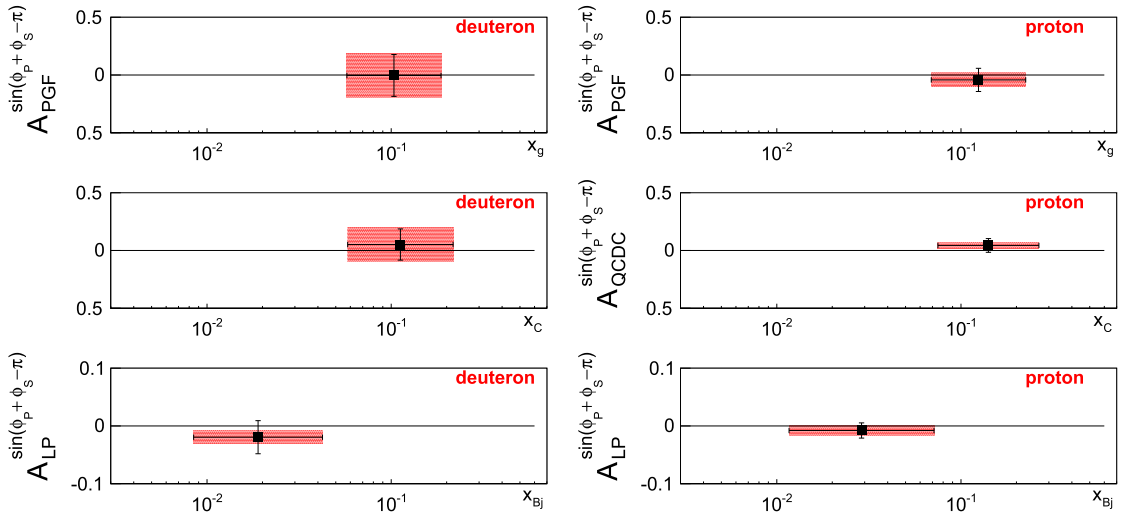

Fig. 8. Collins-like two-hadron asymmetry extracted for Photon–Gluon fusion (PGF), QCD Compton (QCDC) and Leading Process (LP) from the COMPASS two-hadron high-p_T deuteron (left) and proton (right) data. The x range is the RMS of the logarithmic distribution of x in the MC simulation. The red bands indicate the systematic uncertainties. (For interpretation of the references to colour in this figure legend, the reader is referred to the web version of this article.)

function that appears in one process may be different from the one appearing in a different process, so that and assessment of compatibility may require a deeper theoretical analysis.

For the asymmetry of the leading process, the high-p_T sample of the COMPASS proton data has provided a positive value (see Fig. 7 right-bottom panel). It can be compared with the COMPASS results on the Sivers asymmetry for charged hadrons produced in SIDIS $\ell p \to \ell' h^{\pm} X$ single-hadron production [17], which for negative hadrons was found to be about zero and for positive hadrons different from zero and positive, so that for the two-hadron final state a positive value may indeed be expected.

The same analysis method was also applied to extract the Collins-like asymmetry for charged hadrons, *i.e.* the cross section dependence on the sine of the Collins angle $(\phi_P + \phi_S - \pi)$. The asymmetries $A^{\sin(\phi_P+\phi_S-\pi)}_{\rm PGF}$, $A^{\sin(\phi_P+\phi_S-\pi)}_{\rm QCDC}$, $A^{\sin(\phi_P+\phi_S-\pi)}_{\rm LP}$ were determined using the same COMPASS high-p_T deuteron and proton data as used for main analysis in this work. The results are shown in Fig. 8. The amplitude of the Collins modulation for gluons is found to be consistent with zero, in agreement with the naive expectation that is based on the fact that there is no gluon transversity distribution [57]. Recently it was suggested that a transversity-like TMD gluon distribution h_1^g could generate a $\sin(\phi_S + \phi_T)$ modulation in leptoproduction of two jets or heavy quarks [44]. In this case the results shown in Fig. 8 provide a bound on the size of h_1^g. The results given in this letter can also be interpreted such that no false Collins-like asymmetry is introduced by the rather complex analysis method used, so that the non-zero result obtained for the gluon Sivers asymmetry is supported. In addition it is noted that the Collins-like asymmetry of the leading process for the proton is found to be consistent with zero for high-p_T hadron pairs, in qualitative agreement with the measurement of the Collins asymmetry in single-hadron SIDIS measurement [58], where opposite values of about equal size were observed for positive and negative hadrons.

8. Summary and conclusions

The Sivers asymmetry for gluons is extracted from the measurement of high-p_T hadron pairs in SIDIS at COMPASS off transversely polarised deuterons and protons. The analysis is very similar to the one already used by the COMPASS collaboration to measure $\Delta g/g$, the gluon polarisation in a longitudinally polarised nucleon. The large kinematic acceptance of the COMPASS apparatus and the high energy of the muon beam make the sample containing two high-p_T hadrons sufficiently large for the present analysis, which is limited to a small part of the accessible phase space. The criteria applied to select hadron pairs allow us to enhance the contribution of the photon–gluon fusion subprocess with respect to the leading-order virtual-photon absorption subprocess. The Sivers asymmetry is obtained as the amplitude of the sine modulation in the Sivers angle, $\phi_{Siv} = \phi_P - \phi_S$.

The selected high-p_T hadron-pair sample contains already an enriched fraction of events produced in the PGF subprocess. Still, it is necessary to subtract the contributions of the other two subprocesses, LP and QCDC. In this analysis, the fractions of the three subprocesses are determined using MC algorithms, and the three corresponding asymmetries are extracted from the data using a NN technique. Since the results derived from a NN approach strongly depend on the Monte Carlo sample on which the network was trained, the analysis requires a precise MC description of the data. Hence much effort was devoted to obtain a good description of the experimental data by MC simulations. In particular, the analysis was repeated using eight different MC simulations and the (small) differences in the resulting Sivers asymmetries are included in the systematic uncertainties.

Averaging the results obtained from the deuteron and proton data, the measured gluon Sivers asymmetry is obtained as $-0.23 \pm 0.08(\text{stat.}) \pm 0.05(\text{syst.})$, which is away from zero by more than two standard deviations of the total experimental uncertainty. This result supports the possible existence of a non-zero Sivers function, and hence of gluon orbital angular momentum in a transversely polarised nucleon.

In addition, another result obtained in this work is the extraction of the Collins-like gluon asymmetry, *i.e.* the amplitude of the sine modulation of the Collins angle $\phi_{Col} = \phi_P + \phi_S - \pi$. Recent developments have hypothesised a non-zero Collins-like gluon asymmetry, which is however not related to transversity. Our result on the Collins-like asymmetry, which is obtained from the same hadron-pair data that was used to extract the non-zero result on the gluon Sivers asymmetry, is found to be compatible with zero.

Acknowledgements

This work was made possible thanks to the financial support of our funding agencies. We also acknowledge the support of the CERN management and staff, as well as the skills and efforts of the technicians of the collaborating institutes.

References

[1] D.W. Sivers, Phys. Rev. D 41 (1990) 83.
[2] J. Antille, et al., Phys. Lett. B 94 (1980) 523.
[3] FNAL-E704, D.L. Adams, et al., Phys. Lett. B 264 (1991) 462.
[4] E704, E581, D.L. Adams, et al., Phys. Lett. B 261 (1991) 201.
[5] J.C. Collins, Nucl. Phys. B 396 (1993) 161, arXiv:hep-ph/9208213.
[6] S.J. Brodsky, D.S. Hwang, I. Schmidt, Phys. Lett. B 530 (2002) 99, arXiv:hep-ph/0201296.
[7] J.C. Collins, Phys. Lett. B 536 (2002) 43, arXiv:hep-ph/0204004.
[8] HERMES Collaboration, A. Airapetian, et al., Phys. Rev. Lett. 94 (2005) 012002, arXiv:hep-ex/0408013.
[9] COMPASS Collaboration, M.G. Alekseev, et al., Phys. Lett. B 692 (2010) 240, arXiv:1005.5609 [hep-ex].
[10] COMPASS Collaboration, V.Yu. Alexakhin, et al., Phys. Rev. Lett. 94 (2005) 202002, arXiv:hep-ex/0503002.
[11] M. Anselmino, M. Boglione, U. D'Alesio, A. Kotzinian, F. Murgia, A. Prokudin, Phys. Rev. D 72 (2005) 094007, Erratum: Phys. Rev. D 72 (2005) 099903, arXiv:hep-ph/0507181.
[12] W. Vogelsang, F. Yuan, Phys. Rev. D 72 (2005) 054028, arXiv:hep-ph/0507266.
[13] A.V. Efremov, K. Goeke, P. Schweitzer, Eur. Phys. J. Spec. Top. 162 (2008) 1, arXiv:0801.2238 [hep-ph].
[14] HERMES Collaboration, A. Airapetian, et al., Phys. Rev. Lett. 103 (2009) 152002, arXiv:0906.3918 [hep-ex].
[15] COMPASS Collaboration, E.S. Ageev, et al., Nucl. Phys. B 765 (2007) 31, arXiv:hep-ex/0610068.
[16] COMPASS Collaboration, M. Alekseev, et al., Phys. Lett. B 673 (2009) 127, arXiv:0802.2160 [hep-ex].
[17] COMPASS Collaboration, C. Adolph, et al., Phys. Lett. B 717 (2012) 383, arXiv:1205.5122 [hep-ex].
[18] Jefferson Lab Hall A Collaboration, X. Qian, et al., Phys. Rev. Lett. 107 (2011) 072003, arXiv:1106.0363 [nucl-ex].
[19] Jefferson Lab Hall A Collaboration, Y.X. Zhao, et al., Phys. Rev. C 90 (2014) 055201, arXiv:1404.7204 [nucl-ex].
[20] V. Barone, F. Bradamante, A. Martin, Prog. Part. Nucl. Phys. 65 (2010) 267, arXiv:1011.0909 [hep-ph].
[21] C.A. Aidala, S.D. Bass, D. Hasch, G.K. Mallot, Rev. Mod. Phys. 85 (2013) 655, arXiv:1209.2803 [hep-ph].
[22] H. Avakian, A. Bressan, M. Contalbrigo, Eur. Phys. J. A 52 (2016) 150, Erratum: Eur. Phys. J. A 52 (6) (2016) 165.
[23] P.J. Mulders, J. Rodrigues, Phys. Rev. D 63 (2001) 094021, arXiv:hep-ph/0009343.
[24] D. Boer, C. Lorcé, C. Pisano, J. Zhou, Adv. High Energy Phys. 2015 (2015) 371396, arXiv:1504.04332 [hep-ph] and the reference therein.
[25] M. Burkardt, Phys. Rev. D 66 (2002) 114005, arXiv:hep-ph/0209179.
[26] D. Sivers, Phys. Rev. D 74 (2006) 094008, arXiv:hep-ph/0609080.
[27] M. Burkardt, Int. J. Mod. Phys. A 18 (2003) 173, arXiv:hep-ph/0207047.
[28] M. Burkardt, Nucl. Phys. A 735 (2004) 185, arXiv:hep-ph/0302144.
[29] A. Bacchetta, M. Radici, Phys. Rev. Lett. 107 (2011) 212001, arXiv:1107.5755 [hep-ph].
[30] M. Burkardt, Phys. Rev. D 69 (2004) 091501, arXiv:hep-ph/0402014.
[31] M. Anselmino, et al., Eur. Phys. J. A 39 (2009) 89, arXiv:0805.2677 [hep-ph].
[32] S.J. Brodsky, S. Gardner, Phys. Lett. B 643 (2006) 22, arXiv:hep-ph/0608219.
[33] U. D'Alesio, F. Murgia, C. Pisano, J. High Energy Phys. 09 (2015) 119, arXiv:1506.03078 [hep-ph].
[34] PHENIX Collaboration, A. Adare, et al., Phys. Rev. D 90 (2014) 012006, arXiv:1312.1995 [hep-ex].
[35] COMPASS Collaboration, C. Adolph, et al., Phys. Rev. D 87 (2013) 052018, arXiv:1211.6849 [hep-ex].
[36] A. Bravar, D. von Harrach, A. Kotzinian, Phys. Lett. B 421 (1998) 349, arXiv:hep-ph/9710266.
[37] COMPASS Collaboration, C. Adolph, et al., Phys. Lett. B 718 (2013) 922, arXiv:1202.4064 [hep-ex].
[38] COMPASS Collaboration, C. Adolph, et al., sub. Eur. Phys. J. C, arXiv:1512.05053 [hep-ex].
[39] H. Cramer, Mathematical Methods of Statistics, Princeton Univ. Press, Princeton NJ, 1946;
C.R. Rao, Bull. Calcutta Math. Soc. 37 (1945) 81.
[40] COMPASS Collaboration, P. Abbon, et al., Nucl. Instrum. Methods A 577 (2007) 455, arXiv:hep-ex/0703049.
[41] G. Ingelman, A. Edin, J. Rathsman, Comput. Phys. Commun. 101 (1997) 108, arXiv:hep-ph/9605286.
[42] B. Andersson, G. Gustafson, G. Ingelman, T. Sjostrand, Phys. Rep. 97 (1983) 31.
[43] A. Bacchetta, et al., J. High Energy Phys. 02 (2007) 093, arXiv:hep-ph/0611265.
[44] D. Boer, P.J. Mulders, C. Pisano, J. Zhou, J. High Energy Phys. (2016), arXiv:1605.07934 [hep-ph].
[45] J. Pretz, Nucl. Instrum. Methods A 659 (2011) 456, arXiv:1104.1038 [physics.data-an].
[46] A. Szabelski, PhD Thesis, National Centre for Nuclear Research, Warsaw, 2016.
[47] R. Sulej, Netmaker, http://www.ire.pw.edu.pl/~rsulej/NetMaker/.
[48] New Muon Collaboration, M. Arneodo, et al., Nucl. Phys. B 483 (1997) 3, arXiv:hep-ph/9610231.
[49] A.A. Akhundov, D.Y. Bardin, L. Kalinovskaya, T. Riemann, Fortschr. Phys. 44 (1996) 373, arXiv:hep-ph/9407266.
[50] A. Ferrari, P.R. Sala, A. Fasso, J. Ranft, Fluka, http://www.fluka.org, 2005.
[51] M. Bengtsson, T. Sjostrand, Z. Phys. C 37 (1988) 465.
[52] CTEQ Collaboration, H. Lai, et al., Eur. Phys. J. C 12 (2000) 375, arXiv:hep-ph/9903282.
[53] E143 Collaboration, K. Abe, et al., Phys. Lett. B 452 (1999) 194, arXiv:hep-ex/9808028.
[54] H. Fesefeldt, The Simulation of Hadronic Showers: Physics and Applications, 1985.
[55] I. Akushevich, H. Bottcher, D. Ryckbosch, in: Monte Carlo generators for HERA Physics, Proceedings, Workshop, Hamburg, Germany, 1998–1999, 1998, pp. 554–565, arXiv:hep-ph/9906408.
[56] M.G.A. Buffing, A. Mukherjee, P.J. Mulders, Phys. Rev. D 88 (2013) 054027, arXiv:1306.5897 [hep-ph].
[57] V. Barone, A. Drago, P.G. Ratcliffe, Phys. Rep. 359 (2002) 1, arXiv:hep-ph/0104283.
[58] COMPASS Collaboration, C. Adolph, et al., Phys. Lett. B 717 (2012) 376, arXiv:1205.5121 [hep-ex].